International Conference Cybernetics & Informatics 2022
Visegrád, Hungary, September 11th - September 14th, 2022

Hybrid Intelligent MPC In Industry

Peter Karas
Faculty of Electrotechnics and Informatics
Slovak Technical University
Bratislava, Slovak Republic
petokaras@gmail.com

Štefan Kozák
Faculty of Informatics
Pan-European University
Bratislava, Slovak Republic
stefan.kozak@paneurouni.com

***Abstract*— The paper deals with current research challenges in modeling and constrained predictive control as applied to a nonlinear process used in chemical industry (chemical reactor for polypropylene production), and mainly focusing on AI - based or soft computing methods. Based on a combination of the classical approach to modeling of a complex nonlinear process with hybrid dynamics and SC control methods, a prediction model is obtained and subsequently used in the process of solving the optimization problem of constrained predictive control and applied to a simulation model of a reactor used in petrochemical industry.**

Keywords*— *Control engineering, mathematical models, MPC, Model predictive control, chemical plant, petrochemicals, hybrid MPC, neural networks

I. Introduction

The aim of this work is to analyze the possibility of implementing modified advanced control in a petrochemical plant, and to develop an appropriate control method based on soft computing approaches (neural networks).

This work's primary target and purpose are to analyze the possible application of hybrid MPC methods based on the soft computing approach in the industry. The method's application has been simulated and analyzed using the real process data from an existing plant. The process selected for this task is common and essential in the petrochemical industry – polymerization in fluidized bed reactor. This process is nonlinear, affected by inputs and having several internal state variables [2]. The natural advantages of the optimal constrained control method provided by the MPC method may improve optimal plant operation [15]. Even a small improvement of operating condition may provide significant improvement in asset value. The polymerization reactor is online almost entire year, and it is primarily operated in optimal conditions developed by long term operation and experience. Through the comparison of the MPC with neural network observer and mathematical model, we identified the advantages of the optimal constrained control method provided by the MPC with neural observer.

A. Process description

The process selected for this work is a worldwide well-known and frequently used process - the Union Carbide gas-phase polypropylene process (UNIPOL). The UNIPOL process is a result of cooperation between Union Carbide Corporation and Shell chemical [13]. In the latest literature [14] can be found that the heat removal can be partially substituted by some amount of liquid evaporation in the fluidized bed. This principle is frequently called the condensation mode type of cooling. The process is designed for the gas-phase chemical reaction in the fluidized bed. Besides delivering the reactants, the cycle gas does two main functions: it ensures of the reactor bed fluidization and provides mixing to the reactor bed. The cycle gas circulates in the system, while in the cycle is filtered, pressurized by the compressor, cooled down in cycle Gas Cooler and then is returned to the reactor in the bottom section. The gas velocity is an important process parameter and defines optimal reactor bed conditions [6].

The reactor bed fluidization also depends on the particle size. The effect of the particle size on the polymerization reaction has been considered in [9]. The process selected is a polypropylene reactor in the polypropylene plant PP5 in a Slovak petrochemical company. This plant uses an Advanced Process Control system provided by the technology licensor, and the method behind this system is intellectual property of the APC company.

B. Production in the polymerization reactor

In the reactor are produced thirteen different products - thirteen different types of polypropylenes. For the research purposes we decided to select only the best representatives to prove the control system performance. The Impact co-polymers (ICP's) (or Random co-polymers (RCP's)) are produced with additional co-monomer, which means a significant problem for the control system. Due to involvement, the industrial control system must be scalable to provide flexibility and wide range of application. The products selected for the case study are

1. Product 1 - IM 1259
2. Product 2 - HT 306
3. Product 3 - HG 1007

IM 1259 will show the control system's ability to switch to a process with more reactants, while HT 306 and HG 1007 will present the control method scalability. Although the two HPP's (Homo polypropylenes) have the same number of reactants, different operation parameters are required.

II. Modeling and Control Problem Formulation

A. Polymerization reaction

The reaction occurs in the gas phase in the Ziegler – Natta catalyst. The gas stream provides monomer (C3H6), hydrogen (H2), and Catalyst (Ziegler-Natta) to the reactor. The reaction occurs in the pores of Ziegler – Natta catalyst and the presence of co-catalyst together with selectivity control agent. The reactor is stirred ideally by the cycle gas flowing from the bottom to the top of the reactor, and the bed is at the minimum fluidization [8]. Homogenous reaction type has been considered in this study. The difference between homogenous and heterogenous polymerization is discussed by Harmon [16]. It is shown that the solution is scalable to the higher number of states while requiring more computational resources.

978-1-6654-8775-7/22/$31.00 ©2022 IEEE

B. Polymer production rate

The total polymer production rate is then expressed as the molecular weight of monomer and co-polymer multiplied by propagation rate [5].

$$R = M_{WC3}.R_{monomer} + M_{WC2}.R_{co-polymer}, \quad (1)$$

$$R_{co-polymer} = C_{C2}.Y_0(t).k_{pc}(i), \quad i = 1, \quad (2)$$

$$R_{monomer} = C_{C3}.Y_0(t).k_p(i), \quad i = 2 \text{ or } 3, \quad (3)$$

The purity of the reactant gives the stability of the molecular weight constant.

C. Material balance

The reactant material balances are based on the chemical reactions in the reactor [17]. The material balance for the reactants is defined as.

$$V_{FB}.\frac{dC_a(t)}{dt} = F_{in}^{Ca}(t).Cat(i) - k_a(t,i).\left(C_a(t) + \frac{v_{SGV}}{h_{FB}}\right), \; i=1,2 \text{ or } 3, C_a(0) = C_{a0} \quad (4)$$

$$V_{FB}.\frac{dC_{C3}(t)}{dt} = F_{in}^{C3}(t).C_{in}^{C3} - F_{out}^{CG}(t).C_{C3}(t) - C_{C3}(t).\left(k_{im}(t,i).P_0(t) + k_p(t,i).Y_0(t) + k_{fm}(t,i).Y_0(t)\right), \; i=1,2 \text{ or } 3, C_{C3}(0) = C_{C30} \quad (5)$$

$$V_{FB}.\frac{dC_{C2}(t)}{dt} = F_{in}^{C2}(t).C_{in}^{C2} - F_{out}^{CG}(t).C_{C2}(t) - C_{C2}(t).\left(k_{ic}(t,i).P_0(t) + k_{pc}(t,i).Y_0(t) + k_{fcm}(t,i).Y_0(t)\right), \; i=1,2 \text{ or } 3, C_{C2}(0) = C_{C20} \quad (6)$$

$$V_{FB}.\frac{dC_{H2}(t)}{dt} = F_{in}^{H2}(t).C_{in}^{H2} - F_{out}^{CG}(t).C_{H2}(t) - C_{H2}(t).(k_H(t,i).Y_0(t)), \; i=1,2 \text{ or } 3, C_{H2}(0) = C_{H20} \quad (7)$$

The volume flow rates F_{in}^{Ca}, F_{in}^{C3}, F_{in}^{C2} or F_{in}^{H2} are important for the control system. F_{in}^{Ca} is a manipulated variable and F_{in}^{C3}, F_{in}^{C2} or F_{in}^{H2} will be in the position of the measurable disturbance.

$$F_{in}^{Ca} = M_{in}^{Ca}(t).\frac{1}{3600}.\frac{1}{\rho_{Ca}}, \quad (8)$$

$$F_{in}^{C3} = M_{in}^{C3}(t).\frac{1}{3600}.\frac{1}{\rho_{C3}(t).\frac{p_{Rx1}}{p_{atm}}.\frac{T_{atm}}{T_{ref}}}, \quad (9)$$

$$F_{in}^{C2} = M_{in}^{C2}(t).\frac{1}{3600}.\frac{1}{\rho_{C2}(t).\frac{p_{Rx1}}{p_{atm}}.\frac{T_{atm}}{T_{ref}}}, \quad (10)$$

$$F_{in}^{H2} = M_{in}^{H2}(t).\frac{1}{3600}.\frac{1}{\rho_{H2}(t).\frac{p_{Rx1}}{p_{atm}}.\frac{T_{atm}}{T_{ref}}}, \quad (11)$$

The molar concentrations of the reactants on the reactor inlet are considered as measurable disturbance variables and are defined

$$C_{in}^{C3} = \rho_{C3}(t).\frac{1000}{1}.M_w^{C3}, \quad (12)$$

$$C_{in}^{C2} = \rho_{C2}(t).\frac{1000}{1}.M_w^{C2}, \quad (13)$$

$$C_{in}^{H2} = \rho_{H2}(t).\frac{1000}{1}.M_w^{H2}, \quad (14)$$

where the M_w^{C3}, M_w^{C2} and M_w^{H2} are molecular weights of the respective reactants. The concentration of the activated catalyst sites is then defined

$$V_{FB}.\frac{dP_0(t)}{dt} = k_a(t,i).C_a(t) - P_0(t).\left(k_{im}(t,i).C_{C3}(t) + k_{ic}(t,i).C_{C2}(t) + \frac{v_{SGV}}{h_{FB}}\right), \; i=1,2 \text{ or } 3, P_0(0)=P_{00} \quad (15)$$

The concentration of living polymer chains is defined according to several researches works [5 and 8].

$$V_{FB}.\frac{dP_i(t)}{dt} = P_{i-1}(t).\left(k_p(t,i).C_{C3}(t) + k_{pc}(t,i).C_{C2}(t)\right) - P_i(t).\left(k_p(t,i).C_{C3}(t) + k_{fm}(t,i).C_{C3}(t) + k_{pc}(t,i).C_{C2}(t) + k_{fcm}(t,i).C_{C2}(t) + k_H(t,i).C_{H2}(t) + \frac{v_{SGV}}{h_{FB}}\right), \; i=1,2 \text{ or } 3, P_i(0)=P_{i0} \quad (16)$$

According to Eq. (15) and (16), the zeroth moment of the distributions of the polymer chains is then defined

$$V_{FB}.\frac{dY_0(t)}{dt} = \frac{dP_0(t)}{dt} + \sum_{i=2}^{\infty}\frac{dP_i(t)}{dt} = P_0(t).\left(k_p(t,i).C_{C3}(t) + k_{pc}(t,i).C_{C2}(t)\right) - P_i(t).\left(k_p(t,i).C_{C3}(t) + k_{fm}(t,i).C_{C3}(t) + k_{pc}(t,i).C_{C2}(t) + k_{fcm}(t,i).C_{C2}(t) + k_H(t,i).C_{H2}(t) + \frac{v_{SGV}}{h_{FB}}\right) + \sum_{i=2}^{\infty}\left[P_{i-1}(t).\left(k_p(t,i).C_{C3}(t) + k_{pc}(t,i).C_{C2}(t)\right) - P_i(t).\left(k_p(t,i).C_{C3}(t) + k_{fm}(t,i).C_{C3}(t) + k_{pc}(t,i).C_{C2}(t) + k_{fcm}(t,i).C_{C2}(t) + k_H(t,i).C_{H2}(t) + \frac{v_{SGV}}{h_{FB}}\right)\right], \quad i = 1,2 \text{ or } 3 \quad (17)$$

We get the reduced ODE for zeroth moment distributions.

$$V_{FB}.\frac{dY_0(t)}{dt} = P_0(t).\left(k_p(t,i).C_{C3}(t) + k_{pc}(t,i).C_{C2}(t)\right) - Y_0(t).\left(k_{fm}(t,i).C_{C3}(t) + k_{fcm}(t,i).C_{C2}(t) + k_H(t,i).C_{H2}(t) + \frac{v_{SGV}}{h_{FB}}\right), \; i = 1,2 \text{ or } 3, Y_0(0) = Y_0 \quad (18)$$

The gases are cycled through the system, continuously delivering the reactants to the reactor and removing the heat. The reactor's retention time must be considered. For the retention time, we can write

$$\frac{1}{T_{ret}} = \frac{v_{SGV}}{h_{FB}}, \quad (19)$$

where T_{ret} is the retention time, v_{SGV} is the superficial gas velocity in and h_{FB} is the height of the fluidized bed. The first moment of the distributions of the polymer chains are expressed as $Y_1(t)$.

$$V_{FB}.\frac{dY_1(t)}{dt} = P_0(t).\left(k_p(t,i).C_{C3}(t) + k_{pc}(t,i).C_{C2}(t)\right) + Y_0(t).\left(k_{fm}(t,i).C_{C3}(t) + k_{fcm}(t,i).C_{C2}(t)\right) + Y_0(t) - Y_1(t).\left(k_{fm}(t,i).C_{C3}(t) + k_{fcm}(t,i).C_{C2}(t) + k_H(t,i).C_{H2}(t) + \frac{v_{SGV}}{h_{FB}}\right), \; i=1,2 \text{ or } 3, Y_1(0)=Y_{10} \quad (20)$$

we used the definitions in Eq. (21) and Eq. (22)

$$\sum_{i=2}^{\infty} i.(P_{i-1}) = \sum_{i=1}^{\infty}(i+1).(P_i) = Y_1 + Y_0, \quad (21)$$

$$\sum_{i=2}^{\infty} i^2.(P_{i-1}) = \sum_{i=1}^{\infty}(i+1)^2.(P_i) = Y_2 + 2.Y_1 + Y_0, \quad (22)$$

The ODE for second-moment distributions $Y_2(t)$ is

$$V_{FB}.\frac{dY_2(t)}{dt} = P_0(t).\left(k_p(t,i).C_{C3}(t) + k_{pc}(t,i).C_{C2}(t)\right) + Y_0(t).\left(k_{fm}(t,i).C_{C3}(t) + k_{fcm}(t,i).C_{C2}(t)\right) + (2.Y_0(t) + Y_0(t)).\left(k_p(t,i).C_{C3}(t) + k_{pc}(t,i).C_{C2}(t)\right) - Y_2(t).\left(k_{fm}(t,i).C_{C3}(t) + k_{fcm}(t,i).C_{C2}(t) + k_H(t,i).C_{H2}(t) + \frac{v_{SGV}}{h_{FB}}\right), \; i = 1,2 \text{ or } 3, Y_2(0) = Y_{20} \quad (23)$$

The dead polymer chain distributions is defined

$$X_n = \sum_{l=1}^{\infty} l^n . Q_l, \tag{24}$$

The zeroth, first, and second moments of dead polymer distributions are shown in Eq. (25, 26 and 27)

$$\begin{aligned} V_{FB}.\frac{dX_0(t)}{dt} &= Y_0(t).\left(k_{fm}(t,i).C_{C3}(t)\right. \\ &+ k_{fcm}(t,i).C_{C2}(t) \\ &\left.+ k_H(t,i).C_{H2}(t)\right) \\ &- X_0(t).\left(\frac{v_{SGV}}{h_{FB}}\right), \\ &i = 1,2\ or\ 3,\ X_0(0) = X_{00} \end{aligned} \tag{25}$$

$$\begin{aligned} V_{FB}.\frac{dX_1(t)}{dt} &= Y_1(t).\left(k_{fm}(t,i).C_{C3}(t)\right. \\ &+ k_{fcm}(t,i).C_{C2}(t) \\ &\left.+ k_H(t,i).C_{H2}(t)\right) \\ &- X_1(t).\left(\frac{v_{SGV}}{h_{FB}}\right), \\ &i = 1,2\ or\ 3, X_1(0) = X_{10} \end{aligned} \tag{26}$$

$$\begin{aligned} V_{FB}.\frac{dX_2(t)}{dt} &= Y_2(t).\left(k_{fm}(t,i).C_{C3}(t)\right. \\ &+ k_{fcm}(t,i).C_{C2}(t) \\ &\left.+ k_H(t,i).C_{H2}(t)\right) \\ &- X_2(t).\left(\frac{v_{SGV}}{h_{FB}}\right), \\ &i = 1,2\ or\ 3, X_2(0) = X_{20} \end{aligned} \tag{27}$$

Y_m and X_m stands for an m-th moment of the polymer population balances. While Y_m means population balance of living polymer chain and X_m means population balances of inactive, dead polymer chains. The parameter $\frac{\mathbf{v_{SGV}}}{\mathbf{h_{FB}}}$ represents the retention time of the reactants in the reactor.

D. The energy balance

The major material inside is the fluidized bed, and the primary material is the produced pellets of polypropylene resin. $\mathbf{F_{out}^{CG}}.\tilde{\rho}_{CG}(i).c_p^{CG}.(T_{in}-T)$ is the amount of energy that enters and leaves to/from the reactor together with cycle gas.

The cycle gas density depends on the cycle gas composition and pressure, which is different for each product. The systems pressure is controlled by the input streams and cycle gas compressor power. The energy balance [17] of the fluidized bed is defined in Eq. (28)

$$\begin{aligned} &V_{FB}.c_p^{PP}.\rho_{PP}(t)\frac{dT}{dt} \\ &= F_{out}^{CG}.\tilde{\rho}_{CG}(t,i).c_p^{CG}.(T_{in}-T) \\ &+ V_{FB}.A_{FB}.(T_{in}-T) \\ &+ V_{FB}.\left[k_d(t,i).l_d(t).P_0(t).(-H^d(i))\right. \\ &+ k_{im}(t,i).P_0(t).C_{C3}(t).\left(+H^{im}(i)\right) \\ &+ k_{icm}(t,i).P_0(t).C_{C2}(t).\left(+H^{icm}(i)\right) \\ &+ k_H(t,i).Y_0(t).C_{H2}(t).\left(+H^H(i)\right) \\ &+ k_{fm}(t,i).Y_0(t).C_{C3}(t).\left(+H^{fm}(i)\right) \\ &+ k_{fcm}(t,i).Y_0(t).C_{C2}(t).\left(+H^{fcm}(i)\right) \\ &+ k_d(t,i).Y_0(t).\left(-H^d(i)\right) \\ &+ k_{dl}(t,i).Y_0(t).l_d(t).\left(-H^{dl}(i)\right) \\ &+ k_p(t,i).Y_0(t).C_{C3}(t).\left(+H^p(i)\right) \\ &\left.+ k_{pc}(t,i).Y_0(t).C_{C2}(t).\left(+H^{pc}(i)\right)\right], \\ &i = 1,2\ or\ 3, T(0) = T_0 \end{aligned} \tag{28}$$

The total density is calculated from the gas composition.

$$\rho_{CG}(t,i) = \rho_{C3}(t), i = 1 \tag{29}$$

$$\rho_{CG}(t,i) = \frac{V_{C2}.\rho_{C2}(t)+V_{C3}.\rho_{C3}(t).(t)}{V_{C2}+V_{C3}}, i = 2\ or\ 3 \tag{30}$$

The temperature and pressure inside the reactor have to be considered.

$$\tilde{\rho}_{CG}(t,i) = \rho_{CG}(t,i).\frac{p_{Rx1}}{p_{atm}}.\frac{T_{atm}}{T_{ref}}, \tag{31}$$

Eq. (31) shows the normalization of the cycle gas density to the reference pressure and temperature inside the reactor. The term $\mathbf{V_{FB}}.\mathbf{A_{FB}}.(\mathbf{T_{in}}-\mathbf{T})$ represents the energy removed from the system by the heat transfer from the resin to the cycle gas. The last term in the energy balance Eq. 28 is the heat generated by the polymerization reaction. The terms $\mathbf{H}^{\cdots}$ are the enthalpies of the chemical reaction and are specific to the reactants, product, and reaction type. The signing convention has been made while $+\mathbf{H}^{\cdots}$ sign means that the energy has been generated and the sign $-\mathbf{H}^{\cdots}$ means that the energy or heat has been consumed. The polymerization is an exothermic reaction, and therefore most of the heat is generated rather than consumed.

E. The product switching

As mentioned before, to demonstrate the product selectivity, this work considers three different polymers – products in the controller. Several model parameters are product dependent, and in the previous section, the Eq. are denoted as functional of i. The simulations and model tuning has been done for parameters are taken from literature and listed in Tab.1.

TABLE I. PRODUCT PARAMETERS

Prod. 1 (IM 12 59)	Prod. 2 (HT 3 06)	Prod. 3 (HG 10 07)
$k_{a0}(i) = 1$		
$k_{im0}(i) = 22$ [5]	$k_{im0}(i) = 22$ [5]	$k_{im0}(i) = 22$ [5]
$k_{ic0}(i) = 2{,}2$ [11]	$k_{ic0}(i) = 2{,}2$ [11]	$k_{ic0}(i) = 2.2$ [11]
$k_{H0}(i) = 100$		
$k_{fm0}(i) = 100$	$k_{fm0}(i) = 100$	$k_{fm0}(i) = 100$
$k_{fcm0}(i) = 100$	$k_{fcm0}(i) = 0$	$k_{fcm0}(i) = 0$
$k_{d0}(i) = 1000$ [12]		
$k_{dl0}(i) = 1000$ [12]		
$k_{pc0}(i) = 5$	$k_{pc0}(i) = 8$	$k_{pc0}(i) = 30$
$k_{p0}(i) = 2$	$k_{p0}(i) = 0$	$k_{p0}(i) = 0$
$H^a(i) = 7.64$ [11]		
$H^{im}(i) = 7{,}2$ [10]	$H^{im}(i) = 7{,}2$ [10]	$H^{im}(i) = 7{,}2$ [10]
$H^{ic}(i) = 7{,}2$ [10]	$H^{ic}(i) = 7{,}2$ [10]	$H^{ic}(i) = 7{,}2$ [10]
$H^H(i) = 10{,}7$ [10]		
$H^{fm}(i) = 65{,}42$ [10]	$H^{fm}(i) = 65{,}42$ [10]	$H^{fm}(i) = 65{,}42$ [10]
$H^{fcm}(i) = 65{,}42$ [10]	$H^{fcm}(i) = 65{,}42$ [10]	$H^{fcm}(i) = 65{,}42$ [10]
$H^d(i) = 0$		
$H^{dl}(i) = 0$		
$H^{pc}(i) = 7{,}2$ [10]	$H^{pc}(i) = 7{,}2$ [10]	$H^{pc}(i) = 7{,}2$ [10]
$H^p(i) = 10{,}2$ [10]	$H^p(i) = 10{,}2$ [10]	$H^p(i) = 10{,}2$ [10]
$Cat(i) = 10000$	$Cat(i) = 10500$	$Cat(i) = 8000$

The switching between the products is discrete [18]. According to product type state variable, the product-specific rate constants and enthalpies are selected together with catalyst density [4].

F. Hybrid nonlinear MPC

We propose using a neural network for the feedback estimation of the state variables, which are virtual and therefore not measurable by any measuring device [18]. As shown in Fig. 3, the state feedback is separated into two groups of variables. The variables $\mathbf{x}_M(\mathbf{t}) = [\mathbf{C_a}, \mathbf{C_{C3}}, \mathbf{C_{C2}}, \mathbf{C_{H2}}, \mathbf{T}]^{\mathbf{T}}$ and $\mathbf{x}_V(\mathbf{t}) = [\mathbf{P_0}, \mathbf{Y_0}]^{\mathbf{T}}$ represent the feedback states. The state vector represent the molar concentrations of the reactants $\mathbf{C_a}, \mathbf{C_{C3}}, \mathbf{C_{C2}}, \mathbf{C_{H2}}$ and the temperature at which the reaction occurs $\mathbf{T}$. The vector $\mathbf{x}_V(\mathbf{t})$ represent the unmeasurable state vector, which stands for virtual molar concentrations of the active catalyst sites and living polymer chains.

Since a nonlinear MPC controller is a discrete-time controller [18] and the state function is continuous-time, the model gets discretized by the controller using the implicit trapezoidal rule. This method approximates the integration over an interval by breaking the area down into trapezoids

with more easily computable areas. The integration method is based on the summation of partial areas of the trapezoids.

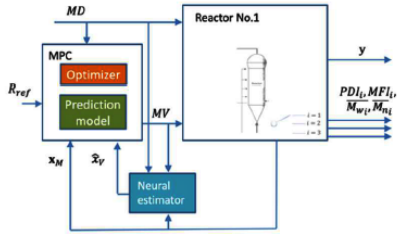


Fig. 1: Simulation model structure with MPC and neural estimator

In Fig. 1 is shown the control structure with a neural estimator for the unmeasurable state variables. The product type, which is the discrete state, determines the type of product and the qualitative properties of PDI and MFI.

G. Hybrid neural estimator

In Fig. 2 is the prediction model as a combination of multiple MLP's.

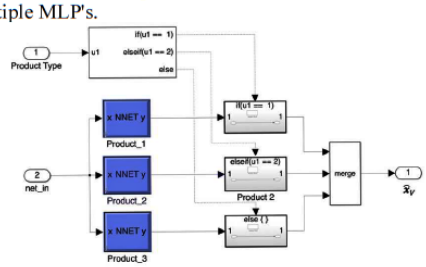


Fig. 2: Prediction model with different MLP for product types

The multiple MLP's shown in Fig. 2 are different neural networks trained with product specific data. Each MLP has its configuration with weights. A good insight into the neural observers and estimators provides Lakhal [20].

H. Control problem formulation

The prediction model is nonlinear. We are interested in controlling the production rate. The output function is defined in Eq. (1). The manipulated variable is the catalyst feed, represented by volume flow defined in Eq. (8). The disturbances are defined as

$$\boldsymbol{M_{DC}}(t) = [F_{in}^{C3}, F_{in}^{C2}, F_{in}^{H2}, T_{in}, v_{SGV}, h_{FB}, p_{Rx1}, \rho_{C3}, \rho_{C2}, \rho_{H2}, \rho_{PP}]^T \quad (32)$$

$$\boldsymbol{M_{DD}}(t) = [\mathrm{i}]^T \quad (33)$$

Eq. (32) shows the continuous signals, while Eq. (33) discrete disturbance – product switching.

The internal states of the prediction model are expressed in Eq. (34).

$$\boldsymbol{x}(t) = [C_a, C_{C3}, C_{C2}, C_{H2}, P_0, Y_0, T]^T \quad (34)$$

The control problem is formulated as minimization of a cost function designed to make the controller's minimum effort to track the reference signal with the output variable. The control problem can be written as defined in Eq. (35).

$$\min_{\boldsymbol{z}(.)} \mathcal{J}\left(\boldsymbol{z}(t), T_c, T_p\right) \quad (35)$$

T_p and T_c are prediction and control horizon with the condition $T_c \leq T_p$ and $\boldsymbol{z}(.)$ is a solution to the optimization problem – a quadratic programming decision.

The objective function J, also called the cost function, is the sum of individual terms, which each focus on the specific aspect of the controller performance [15]. The objective function is formulated in Eq. (36, 37 and 38).

$$\mathcal{J}(\boldsymbol{z}(k)) = \mathcal{J}_y(\boldsymbol{z}(k)) + \mathcal{J}_{\Delta u}(\boldsymbol{z}(k)) \quad (36)$$

$$\mathcal{J}_y(\boldsymbol{z}(k)) = \sum_{i=1}^{\tau_p} \{w_i^y \cdot [r(k+i|k) - y(k+i|k)]\}^2 \quad (37)$$

$$\mathcal{J}_{\Delta u}(\boldsymbol{z}(k)) = \sum_{i=0}^{\tau_p - 1} \{w_i^{\Delta u} \cdot [u_j(k+i|k) - u_j(k+i-1|k)]\}^2 \quad (38)$$

The proposed nonlinear programming solver presented in this thesis is the active set algorithm [21]. The method is based on solving the Kuhn-Tucker equations using SQP principles [21]. The SQP algorithm executed each sample period finds a solution to the quadratic optimization problem defined in Eq. (35). The solution represents an optimal manipulated variable sequence.

The output of the prediction model and manipulated variable are constrained with the condition shown in Eq. (39).

$$R := \{y(t) \in \mathbb{R}^1 | 0\, t.h^{-1} \leq y \leq 50\, t.h^{-1}\}$$

$$U := \begin{Bmatrix} u(t) \in \mathbb{R}^1 | 0\, m^3.h^{-1} \leq u \leq 200\, m^3.h^{-1} \\ -2\, kg.h^{-1} \leq \Delta u \leq 2\, kg.h^{-1} \end{Bmatrix}$$

$$X := \{\boldsymbol{x}(t) \in \mathbb{R}^{12} | -\infty \leq \boldsymbol{x} \leq \infty\} \quad (39)$$

The first step of the sequence is applied to the process, and the process repeats each sampling period.

III. Case Study

The simulations have been done with the step change of a disturbance signal. In Tab.2 is listed an overview of what step changes have been conducted to check the mathematical model performance. The arrows represent the direction of signal change.

TABLE II. STEP CHANGES OF MEASURED DISTURBANCES

Variable/disturbance signal name […]	Time [s]
Superficial gas velocity	2250 ↑,3250 ↓
The actual level of fluidized bed	4250 ↑,5250 ↓
Reactor gas cap pressure	6250 ↑,7250 ↓
Cycle gas specific gravity	8250 ↑,9250 ↓
Polypropylene density	10250 ↑,11250 ↓
Hydrogen density	12250 ↑,13250 ↓
Ethylene density	14250 ↑,15250 ↓
Ethylene volume flow rate into the reactor	16250 ↑,17250 ↓
Hydrogen volume flow rate into the reactor	18250 ↓,19250 ↑
Propylene volume flow rate into the reactor	21250 ↓,22250 ↑
Cycle gas temperature at the reactor inlet	24250 ↑,25250 ↓

The results representing the testing and verification scenario summarized in Tab. 2 are shown in Fig. 3. To verify the inteligent control system design, we propose a set of verification criteria, which will result in the final statement and best candidate.

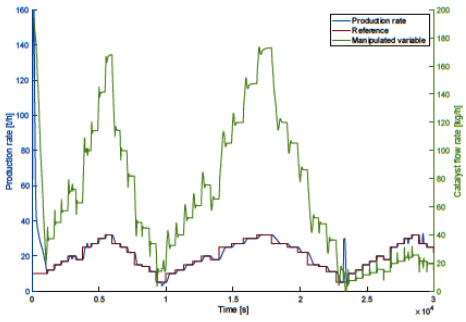


Fig. 3: Step response to the changes

IV. CONCLUSION

A. Verification and results

The controller parameters that characterize the best candidates are sampling period, prediction horizon, and control horizon. The following criteria are evaluated in this section:

1. Compensation of the measurement noise
2. Compensation of the measurement disturbance
3. Transient state stability
4. Manipulated variable stability and manipulator work required
5. Computational requirements and effect of prediction and control horizon
6. Reference tracking

The comparison between the mathematical and neural model with three dedicated neural networks is shown in Fig. 4.

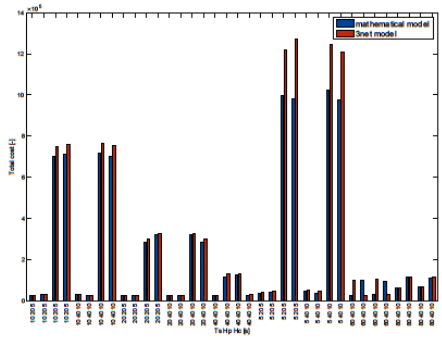


Fig. 4: Mathematical and neural network prediction performance comparison

In Fig. 4 shows better performance of the neural network version (3net) than the mathematical version for specific sample times and prediction/control horizon. The total cost is calculated as the sum of all qualitative parameters. Lower value means better performance, shorter time for execution, or less energy needed by the manipulator.

The critical quality criteria is the reference tracking ability and energy required to manipulate the regulator. The best alternatives are shown in Tab. 3.

TABLE III. BEST CONFIGURATION ACC. TO REF. TRACKING AND ENERGY REQUIREMENTS

Alternative (Cost)	Sampling Period [s]	Prediction Horizon [samples]	Control Horizon [samples]
1 (22101)	20	20	5
2 (22103)	20	40	10
3 (23846)	10	40	10
4 (23923)	10	20	5
5 (27307)	40	40	10

The alternatives 1 and 2 can be considered equally good in terms of reference tracking ability and energy requirements.

The computational time needed for the simulation is a function of neural network complexity and reflects the cost of effort needed for the required accuracy by MPC. This qualitative parameter has been included in the evaluation to present the effect of neural network size and the computational requirements. The best alternatives are shown in Tab. 4.

TABLE IV. ALTERNATIVES ACC. TO REF. TRACKING AND COMPUTATIONAL REQUIREMENTS

Alternative (Cost)	Sampling Period [s]	Prediction Horizon [samples]	Control Horizon [samples]
1 (22293)	20	20	5
2 (22982)	20	40	10
3 (25815)	10	40	10
4 (26898)	10	20	5
5 (27692)	40	40	10

The difference between alternative 1 and 2 has widened, and the best candidate became alternative 1.

Therefore, the quality evaluation and the best candidate selection were also compared according to energy and computational requirements. The best alternatives are shown in Tab. 5.

TABLE V. ALTERNATIVES ACC. TO ENERGY AND COMPUTATIONAL REQUIREMENTS

Alternative (Cost)	Sampling Period [s]	Prediction Horizon [samples]	Control Horizon [samples]
1 (310)	80	40	10
2 (465)	60	40	10
3 (614)	20	20	5
4 (719)	40	40	10
5 (778)	80	40	10

The difference between alternative 1 and 2 has widened, and the best candidate became alternative 1. According to evaluation criteria, the optimal configuration of the MPC for the specific system – polypropylene reactor is the predictive model controller with a sampling period of the 20s, prediction horizon of 20 samples and control horizon of 5 samples.

B. Selecting sampling period, prediction horizon and control horizon

The sampling period of the controller has a significant effect on the overall performance of the closed-loop response [19]. The sampling period effect has been checked with several MPC configurations and prediction and control horizons. The results are different for experiments with measurement noise applied to the feedback signals and situations without any noise. In Fig. 5 and Fig. 6 we show the effect of varying sampling periods on the qualitative parameters.

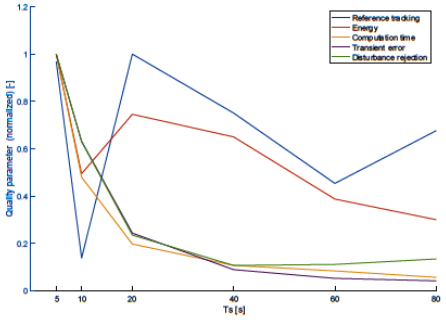


Fig. 5: Sampling period effect on MPC configuration without noise

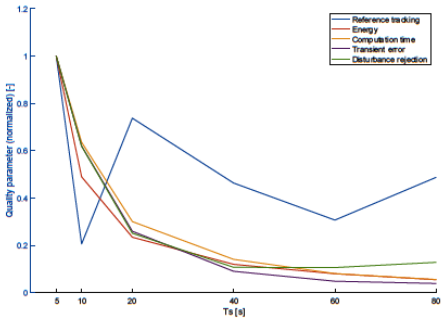


Fig. 6: Sampling period effect on MPC configuration with random noise

The article provides an insight into the kinetic modeling of the specific chemical reaction. It is shown that the approach to the mathematical modeling of the kinetic process during the polymerization reaction is generally applicable in the control theory [5]. An application of the kinetic model for MPC of a highly nonlinear process with discrete states is shown [5]. The article proposes a solution to the control problem using a hybrid controller, which uses neural networks to predict and model the non-measurable states and presents a solution to the discrete states in a hybrid prediction model with discrete sub-model switching. Another achievement to be considered is the scalability and flexibility of the proposed control system. An analysis of the controller performance for multiple system configurations has been conducted again. The numerous neural networks' advantage compared to a single-network solution has been proven and analyzed using objective criteria.

Implementation of the ANN for feedback estimation can eliminate the current heuristic approach, which is highly dependent on the operator. Manual input of the process control can be reduced and thus increase the effectivity and safety.

ACKNOWLEDGMENT

Research on Advanced Algorithms and Process Modelling in Domains of Applied Informatics (RAPDAI)
Grant Agency: Grant Agency Academia Aurea (GAAA)
Project number: GAAA/2022

REFERENCES

[1] Karas, P., Kozák, Š., 2017, Artificial neural network approach to modeling of polypropylene reactor, In International Journal of Advances in Chemistry (IJAC), Vol.3, No. 3, p. 22 - 30
[2] Karas, P., Kozák,, Š., 2018, Highly nonlinear process model using optimal artificial neural network, In Cybernetics and Informatics, 29th International conference proceedings, IEEE catalog number: CFP18E30-PRT, ISBN: 978-1-5386-4419-5, Vol. 19, p. 14 – 22
[3] Shamiri, A. et al., 2015, Modified two-phase model with hybrid control for gas phase propylene copolymerization in fluidized bed reactor, In 2015 Chemical Engineering Journal, No. 264, p. 706 – 719
[4] Karas, P., Kozák,, Š., 2019, Nonlinear process prediction using neural network model, In 2019 ELITECH, 21-th Conference of Doctoral Students, 29 May 2019, FEI STU, Bratislava, Slovakia, p. 8 - 14
[5] Shamiri, A. et al., 2010, Kinetic modeling of propylene homo polymerization in gas-phase fluidized-bed reactor, In Chemical Engineering Journal, Vol. 161, p. 240-249
[6] Shamiri, A. et al., 2013, Dynamics and Predictive Control of Gas Phase Propylene Polymerization in Fluidized Bed Reactors, In Process Systems Engineering and Process Safety, Chemical Journal of Chemical Engineering, Vol. 21, 2013, pp. 1015-1029
[7] Shamiri, A. et al., 2011, Temperature Control of Industrial Gas Phase Propylene Polymerization in Fluidized Bed Reactors Using Model Predictive Control, In 3rd International Conference on Chemical, Biological and Environmental Engineering, IPCBEE, Vol. 20, p. 19 - 24
[8] Ibrehem, A.S. et al., 2008, Mathematical Model and Advanced Control for Gas-phase Olefin Polymerization in Fluidized-bed Catalytic Reactors, Chinese Journal of Chemical Engineering, Vol. 16, p. 84 – 89
[9] Kim, J. Y., 1998, Particle size distribution and its effect on the olefin polymer reactor dynamics over olefin polymerization catalysts with multiple active sites, In Korea J. Chem. Eng., Vol. 15, No. 4, p. 451-457
[10] Luo, Z.-H. et al., 2009, Steady – state and dynamic modeling of commercial bulk polypropylene process of Hypol technology, In Chemical engineering journal, Vol. 149, p. 370 – 382
[11] Bai, F., et al., 2003, Physical Constants of Poly(propylene), The Wiley Database of Polymer Properties
[12] Alshaiban, A., 2008, Active site identification and modeling of polypropylene made with Ziegler – Natta catalysts
[13] Ibrehem, A.S. et al., 2009, Advanced Control of a Fluidized Bed Using a Model-predictive Controller, Australian Journal of Basic od Applied Sciences, Vol. 3, No. 4, p. 3954 - 3974
[14] Ibrehem, A.S. et al., 2008, Decentralized Advanced Model Predictive Controller of Fluidized-Bed for Polymerization Process, Iran. J. Chem. Chem. Eng., Vol. 31, No. 4, p. 91 – 117
[15] Mikleš J., Fikar M., 2004, Modelovanie, identifikácia a riadenie procesov II, Ed. 1
[16] Harmon Ray, W. 1972, On the Mathematical Modeling of Polymerization Reactors, In Journal of Macromolecular Science, Part C, Vol. 8:1, p. 1-56
[17] Lona, L. M. F., 2018, A step by step approach to the modelling of chemical engineering processes, Springer International Publishing AG
[18] Lunze, J., Lamnabhi-Lagarrigue, F., 2009, Handbook of Hybrid Systems Control Theory, Tools, Applications, Cambridge University Press, ISBN-13 978-0-511-64178-7
[19] Kozák, Š., 2003, Development of Advanced Control Methods and Their Successful Incorporation in the Industry, In Journal of Cybernetics and Informatics, ISSN 1336 - 4774, Vol. 1
[20] Lakhal, A.H. et al., 2010, Neural Network Observer for Nonlinear Systems Application to Induction Motors, International Journal of Control and Automation, Vol. 3, No. 1
[21] www.mathworks.com – Matlab SW package reference manual

TABLE VI: NOMENCLATURE AND USED SYMBOLS

Variable	Explanation
V_{FB}	Fluidized bed volume $V_{FB} = \pi . r_{Rx1}^2 . h_{FB} . (1 - \varepsilon_{mf})$ $[m^3]$
$C_a(t)$	The molar concentration of catalyst particles in reactor $[mol.m^{-3}]$
$F_{in}^{Ca}(t)$	Catalyst volume flow rate into the reactor $[m^3.h^{-1}]$
$Cat(i)$	The molar concentration of catalyst particles at reactor inlet $[mol.m^{-3}]$
$k_a(t,i)$	The activation reaction rate constant $[s^{-1}]$
$v_{SGV}(t)$	Superficial gas velocity $[m.s^{-1}]$

$h_{FB}(t)$	The actual level of fluidized-bed [m]
$C_{C3}(t)$	The molar concentration of propylene in reactor $[mol.m^{-3}]$
$F_{in}^{C3}(t)$	Propylene volume flow rate into the reactor $[m^3.h^{-1}]$
C_{in}^{C3}	The molar concentration of propylene at reactor inlet $[mol.m^{-3}]$
$F_{out}^{CG}(t)$	Cycle gas volume flow $[m^3.s^{-1}]$
$k_{im}(t,i)$	Initiation by propylene reaction rate constant $[m^3.mol^{-1}.s^{-1}]$
$P_0(t)$	Active site concentration $[mol.m^{-3}]$
$k_p(t,i)$	Propagation by monomer reaction rate constant $[m^3.mol^{-1}.s^{-1}]$
$Y_0(t)$	0-th moment of living polymer chains $[mol.m^{-3}]$
$k_{fm}(t,i)$	Transfer to propylene reaction rate constant $[m^3.mol^{-1}.s^{-1}]$
$C_{C2}(t)$	The molar concentration of ethylene in reactor $[mol.m^{-3}]$
$F_{in}^{C2}(t)$	Ethylene volume flow rate into the reactor $[m^3.h^{-1}]$
C_{in}^{C2}	The molar concentration of ethylene at reactor inlet $[mol.m^{-3}]$
$k_{ic}(t,i)$	Initiation by ethylene reaction rate constant $[m^3.mol^{-1}.s^{-1}]$
$k_{pc}(t,i)$	Propagation by ethylene reaction rate constant $[m^3.mol^{-1}.s^{-1}]$
$k_{fcm}(t,i)$	Transfer to ethylene reaction rate constant $[m^3.mol^{-1}.s^{-1}]$
$C_{H2}(t)$	The molar concentration of hydrogen in reactor $[mol.m^{-3}]$
$F_{in}^{H2}(t)$	Hydrogen volume flow rate into the reactor $[m^3.s^{-1}]$
C_{in}^{H2}	The molar concentration of hydrogen at reactor inlet $[mol.m^{-3}]$
$k_H(t,i)$	Transfer to hydrogen reaction rate constant $[m^3.mol^{-1}.s^{-1}]$
$M_{in}^{Ca}(t)$	Catalyst mass flow rate into the reactor $[kg.h^{-1}]$
ρ_{Ca}	Catalyst suspension density $[kg.m^{-3}]$
$M_{in}^{C3}(t)$	Propylene mass flow rate into the reactor $[kg.h^{-1}]$
$\rho_{C3}(t)$	Propylene density $[kg.m^{-3}]$
p_{Rx1}	Reactor gas cap pressure [bar]
p_{atm}	Atmospheric pressure [bar]
T_{atm}	Atmospheric temperature [K]
T_{ref}	Reference temperature [K]
$M_{in}^{C2}(t)$	Ethylene mass flow rate into the reactor $[kg.h^{-1}]$
$\rho_{C2}(t)$	Ethylene density $[kg.m^{-3}]$
$M_{in}^{H2}(t)$	Hydrogen mass flow rate into the reactor $[kg.h^{-1}]$
$\rho_{H2}(t)$	Hydrogen density $[kg.m^{-3}]$
M_w^{C3}	The molecular weight of propylene $[kg.kmol^1]$
M_w^{C2}	The molecular weight of ethylene $[kg.kmol^1]$
M_w^{H2}	The molecular weight of hydrogen $[kg.kmol^1]$
$P_1(t)$	Active site concentration with the length of 1 $[mol.m^{-3}]$
$P_l(t)$	Active site concentration with the length of l $[mol.m^{-3}]$
T_{ret}	Reactor retention time [s]
$Y_1(t)$	The first moment of living polymer chains $[mol.m^{-3}]$
$Y_2(t)$	The second moment of living polymer chains $[mol.m^{-3}]$
$X_0(t)$	0-th moment of dead polymer chains $[mol.m^{-3}]$
$X_1(t)$	The first moment of dead polymer chains $[mol.m^{-3}]$
$X_2(t)$	The second moment of dead polymer chains $[mol.m^{-3}]$
c_p^{PP}	Specific heat capacity of polypropylene at 342 K $[J.mol^{-1}.K^{-1}]$
$\rho_{PP}(t)$	Polypropylene density $[kg.m^{-3}]$
$T(t)$	The temperature in the reactor [K]
$\tilde{\rho}_{CG}(t,i)$	Cycle gas specific gravity $[kg.m^{-3}]$
T_{in}	Cycle gas temperature at the reactor inlet [K]
A_{FB}	Cycle gas to fluidized bed heat transfer coefficient
$-H^d(i)$	The heat of reaction – deactivation $[J.mol^{-1}]$
$+H^{im}(i)$	The heat of reaction – initiation by propylene $[J.mol^{-1}]$
$+H^{icm}(i)$	The heat of reaction – initiation by ethylene $[J.mol^{-1}]$
$+H^{H}(i)$	The heat of reaction – transfer to hydrogen $[J.mol^{-1}]$
$+H^{fm}(i)$	The heat of reaction – transfer to propylene $[J.mol^{-1}]$
$+H^{fcm}(i)$	The heat of reaction – transfer to ethylene $[J.mol^{-1}]$
$-H^{dl}($	The heat of reaction –reaction poisoning $[J.mol^{-1}]$
$+H^{p}(i)$	The heat of reaction –propagation by propylene block $[J.mol^{-1}]$
$+H^{pc}(i)$	The heat of reaction –propagation by ethylene block $[J.mol^{-1}]$
ε_{mf}	The void fraction at minimum fluidization [-]
$\rho_{H2}(t)$	Hydrogen density $[kg.m^{-3}]$

Authors



Ing. Peter Karas, PhD.
petokaras@gmail.com
He finished his studies at the Faculty of Electrical Engineering and Information Technology in the field of Automation and Control in 2005. In 2021, he completed his doctoral studies in the field of modeling, simulation and control of non-linear systems through artificial intelligence methods. Currently he works as a project engineering manager in Slovenské elektrárne a.s. (Slovak powerplants company). His main interest is the management and technical preparation of investment projects for conventional and nuclear power plants.



prof. Ing. Štefan Kozák, PhD.
Faculty of Informatics, Pan-European University, Bratislava, Slovakia
stefan.kozak@paneurouni.eu
Currently at the Institute of Applied Informatics at the Faculty of Informatics, Pan-European University in Bratislava. His research interests include system theory, linear and nonlinear control methods, numerical methods and software for modeling, control, signal processing, IoT, IIoT and embedded intelligent systems for digital factory in automotive industry.